

University of Groningen

Synergistic immunomodulatory effect in macrophages mediated by magnetic nanoparticles modified with miRNAs

Lafuente-Gómez, Nuria; Wang, Shiqi; Fontana, Flavia; Dhanjani, Mónica; García-Soriano, David; Correia, Alexandra; Castellanos, Milagros; Rodriguez Diaz, Ciro; Salas, Gorka; Santos, Hélder A.

Published in:
Nanoscale

DOI:
[10.1039/D2NR01767A](https://doi.org/10.1039/D2NR01767A)

IMPORTANT NOTE: You are advised to consult the publisher's version (publisher's PDF) if you wish to cite from it. Please check the document version below.

Document Version
Publisher's PDF, also known as Version of record

Publication date:
2022

[Link to publication in University of Groningen/UMCG research database](#)

Citation for published version (APA):

Lafuente-Gómez, N., Wang, S., Fontana, F., Dhanjani, M., García-Soriano, D., Correia, A., Castellanos, M., Rodriguez Diaz, C., Salas, G., Santos, H. A., & Somoza, A. (2022). Synergistic immunomodulatory effect in macrophages mediated by magnetic nanoparticles modified with miRNAs. *Nanoscale*, 14(31), 11129-11138. <https://doi.org/10.1039/D2NR01767A>

Copyright

Other than for strictly personal use, it is not permitted to download or to forward/distribute the text or part of it without the consent of the author(s) and/or copyright holder(s), unless the work is under an open content license (like Creative Commons).

The publication may also be distributed here under the terms of Article 25fa of the Dutch Copyright Act, indicated by the "Taverne" license. More information can be found on the University of Groningen website: <https://www.rug.nl/library/open-access/self-archiving-pure/taverne-amendment>.

Take-down policy

If you believe that this document breaches copyright please contact us providing details, and we will remove access to the work immediately and investigate your claim.



Cite this: *Nanoscale*, 2022, **14**, 11129

Received 31st March 2022

Accepted 14th July 2022

DOI: 10.1039/d2nr01767a

rsc.li/nanoscale

Synergistic immunomodulatory effect in macrophages mediated by magnetic nanoparticles modified with miRNAs†

Nuria Lafuente-Gómez,  *^a Shiqi Wang,  ^b Flavia Fontana, ^b Mónica Dhanjani,^a David García-Soriano,^a Alexandra Correia,^b Milagros Castellanos,^a Ciro Rodriguez Diaz,  ^a Gorka Salas,  ^{a,c} Hélder A. Santos^{*a,d} and Álvaro Somoza^{*a,c}

In this work, we describe the synthesis of magnetic nanoparticles composed of a maghemite core (MNP) and three different coatings (dextran, D-MNP; carboxymethyl-dextran, CMD-MNP; and dimer-captosuccinic acid, DMSA-MNP). Their interactions with red blood cells, plasma proteins, and macrophages were also assessed. CMD-MNP was selected for its good biosafety profile and for promoting a pro-inflammatory response in macrophages, which was associated with the nature of the coating. Thus, we proposed a smart miRNA delivery system using CMD-MNP as a carrier for cancer immunotherapy applications. Particularly, we prove that CMD-MNP-miRNA155 and CMD-MNP-miRNA125b nanoparticles can display a pro-inflammatory response in human macrophages by increasing the expression of CD80 and the levels of TNF- α and IL-6. Hence, our proposed miRNA-delivery nanosystem can be exploited as a new immunotherapeutic tool based on magnetic nanoparticles.

Introduction

Nanomedicine has attracted tremendous attention for the overwhelming evidence that supports the potential of nano-

particles to improve the safety and efficacy of treatments (*e.g.*, cancer).^{1–3} A wide variety of nanoparticles have been developed for biomedical purposes for years.^{4–7} In this sense, magnetic nanoparticles, composed of metals and/or oxide metals, can be easily synthesized with inexpensive procedures suitable for large-scale production,⁸ their magnetic properties have been explored for diagnostic and therapeutic purposes,^{9–12} and they have been studied for controlled drug release applications.^{13–16} Interestingly, they also display self-adjuvating properties that can be exploited to promote further or modulate the immune function.¹⁷ Another aspect to consider is the importance of evaluating the nanomaterials' interactions with the blood constituents to ensure their biocompatibility.^{18,19}

It is known that a complex and multifaceted relationship between cancer and the immune system exists, and the interplay among them determines the control or spreading of the disease.^{20,21} Noteworthy, tumor-associated macrophages, which are tumor-enriched immunosuppressive cells, play an essential role in cancer development, proliferation and dissemination.^{22,23} Hence, promoting a pro-inflammatory effect on macrophages, also known as M1 state, is a plausible therapeutic approach to combat tumors.²⁴ In this scenario, miRNAs play a crucial role in the innate and adaptive immune system.^{25,26} They are a group of small non-coding RNAs (20–25 nucleotide-long) that act at the post-transcriptional level in the regulation of gene expression.^{25,27,28} Particularly, miRNA-155 and miRNA-125b are known for promoting a pro-inflammatory response of macrophages,^{25,29,30} and miRNA146a is known for its opposite effect.^{31,32} Thus, the delivery of miRNAs can be employed to epigenetically modified these cells towards an active state with high interest for immunotherapeutic applications in cancer treatment.^{33–35}

In this work, we described the synthesis and characterization of maghemite magnetic nanoparticles (MNP) with different coatings (dextran, D-MNP; carboxymethyl-dextran, CMD-MNP; and dimer-captosuccinic acid, DMSA-MNP), and assessed their hemocompatibility, their interactions with plasma proteins and immunotoxicity in murine and human

^aInstituto Madrileño de Estudios Avanzados en Nanociencia (IMDEA Nanociencia), 28049 Madrid, Spain. E-mail: nuria.lafuente@imdea.org, alvaro.somoza@imdea.org

^bDrug Research Program, Division of Pharmaceutical Chemistry and Technology, Faculty of Pharmacy, University of Helsinki, FI-00014 Helsinki, Finland

^cUnidad de Nanobiotecnología Asociada al Centro Nacional de Biotecnología (CSIC), 28049 Madrid, Spain

^dDepartment of Biomedical Engineering, W.J. Kolff Institute for Biomedical Engineering and Materials Science, University Medical Center Groningen/University of Groningen, Ant. Deusinglaan 1, 9713 AV Groningen, The Netherlands. E-mail: h.a.santos@umcg.nl

† Electronic supplementary information (ESI) available: Details on materials and methods, DLS characterization of the formulations, characterization data of nanoparticles (TEM, XRD, TGA), hydrodynamic size evaluation in different media, protein corona evaluation *via* SDS-PAGE and AFM, study of the endocytic pathways involved in the internalization of the nanoparticles, quantification of ROS levels, and cell cycle analysis of macrophages. See DOI: <https://doi.org/10.1039/d2nr01767a>

macrophages to stress the importance of knowing the biosafety profile of nanomaterials. Additionally, their immunomodulatory properties in macrophages were assessed in terms of the expression of co-stimulatory cell surface markers (CD80, CD86) and pro-inflammatory cytokines (TNF- α , IL-6). Moreover, considering the great potential of these nanostructures for the delivery of molecules of interest, we proposed a smart miRNA delivery system with magnetic nanoparticles based on disulfide bonds for the polarization of macrophages. The use of disulfide bonds to anchor molecules of interest to nanoparticles has been widely studied, mainly because it ensures the stability of the complex in blood circulation and extracellular media where the levels of glutathione are remarkably lower than inside cells,^{13,36,37} and it has been harnessed to release cargos also in immune cells.^{38,39} Particularly, the endocytic pathway of antigen presenting cells, which include macrophages, is adapted to reduce the disulfide bonds of proteins to facilitate antigen processing and presentation.⁴⁰ In fact, these cells express gamma interferon-inducible lysosomal thiolreductase (GILT) that reduces disulfide bonds in late endosomes and lysosomes.⁴¹ Overall, these studies will provide insights on the potential of magnetic nanoparticles for their use in biomedical applications at different levels, including their biosafety profile and immunomodulatory properties in macrophages.

Results and discussion

Magnetic nanoparticles were prepared by coprecipitation.^{42,43} They had a mean size of 14 nm (Fig. S1A[†]) and were composed of a core of maghemite (γ -Fe₂O₃, MNP) as indicated in the DRX graph (Fig. S1B[†]). Then, they were coated with dextran (D-MNP), carboxymethyl-dextran (CMD-MNP) or dimercaptosuccinic acid (DMSA-MNP). The resulting nanoparticles maintained their magnetic core intact (Fig. S1C[†]) and the coating efficiency was studied by thermogravimetry (Fig. S1D[†]). They were stable colloidal formulations with a hydrodynamic size ~100 nm but different surface charge (Table S4[†]). Uncoated maghemite cores (MNP) were positively charged, whereas coated samples were negatively charged. The carboxylic acid moieties of DMSA and CMD are responsible for a more negative charge than the hydroxyl groups of dextran. Additionally, their stability was evaluated in PBS, complete DMEM and complete RPMI for 72 h under stirring conditions (Fig. S2[†]). The results revealed that MNP aggregated at all times tested in PBS, and those aggregates (>1000 nm) were also observed with DMSA-MNP after 5 h of incubation. Remarkably, all the nanoparticles maintained a similar hydrodynamic size over time in DMEM and RPMI, although a tendency of aggregation after 24 h of incubation in DMEM was observed with D-MNP, and at the same time in RPMI with DMSA-MNP. The higher aggregation of D-MNP in DMEM could be related to the higher content of ions in comparison with RPMI that interferes with the weak electrostatically repulsion forces among dextran molecules,⁴⁴ whereas the higher aggregation of DMSA-MNP in RPMI might be related to the content of phosphate ions,

which is ~5-fold higher in RPMI vs. DMEM.⁴⁴ In summary, CMD-MNP were the most stable nanoparticles in all media tested.

To ensure the safe use of nanoparticles, it is crucial to assess their biocompatibility with blood components.^{18,19} Consequently, a hemolysis assay was conducted to evaluate the impact of nanoparticles' surface chemistry on red blood cells (RBC) by incubating them for 1 h (0.01–2 mg Fe per mL) in physiological conditions (PBS, pH 7.4, 37 °C), as described elsewhere.^{45,46} The results suggest a high hemotoxicity produced by MNP (Fig. 1A) in comparison with the coated nanoparticles (less than 5%) (Fig. 1B). A plausible explanation is that MNP agglomerate and interact heavily in the form of large clusters with RBC membranes. On the contrary, the presence of the coatings results in electrostatic repulsions between particles, which increases their stability in aqueous solutions.⁴⁷ Additionally, we examined the impact of the coated magnetic nanoparticles on the RBC morphology, which must be unaffected to maintain their physiological function,^{43,48} at two concentrations (0.01 and 0.1 mg Fe per mL) (Fig. 1C). The morphological changes of the RBC surfaces were remarkable with DMSA-MNP, showing a relevant membrane wrapping and shrinkage in a dose-dependent manner. Lastly, new hemolysis assays were performed to check if the morphological alterations observed after 1 h of incubation were translated into the destruction of RBC at longer incubation times (4 h and 24 h) (Fig. 1D). We observed that the hemolysis produced depended on time and concentration. Altogether, these studies revealed the differences in hemocompatibility among the nanoparticles in the following order: D-MNP > CMD-MNP > DMSA-MNP > MNP.

Then, we evaluated the interaction of magnetic nanoparticles with plasma proteins by incubating them with human serum (HS) and checking the formation of a protein corona by SDS-PAGE (Fig. S3A–S3C[†]) and AFM imaging (Fig. S3D[†]). By SDS-PAGE, we found that the MNP avoided the attachment of proteins, whereas the coating of the nanoparticles (D-MNP, CMD-MNP and DMSA-MNP) seemed to promote the interactions with those molecules (Fig. S3A[†]) and that the adsorption of human serum albumin (HSA; the most abundant protein in plasma)⁴⁹ was concentration dependent (Fig. S3B[†]). In our case, the interactions of MNP and plasma proteins were probably hampered by the agglomeration of the nanoparticles in the media due to the PBS (see Fig. S2[†]). Remarkably, when we calculated the percentage of HSA attached in comparison with the percentage of HS added, we concluded that it represented less than 15% (Fig. S3C[†]). Thus, these experiments suggest that the interaction of the plasma proteins with the nanoparticles is limited.

Complementarily, we assessed the size and shape of the final nanostructures by AFM (Fig. S3D[†]). Particularly, DMSA-MNP and especially MNP led to large aggregates. It is worth noting the presence of free plasma proteins in the sample incubated with CMD-MNP. This could be related to the formation of a soft corona due to weak interactions, compared to the stable hard corona,^{50,51} which seems to be the case for

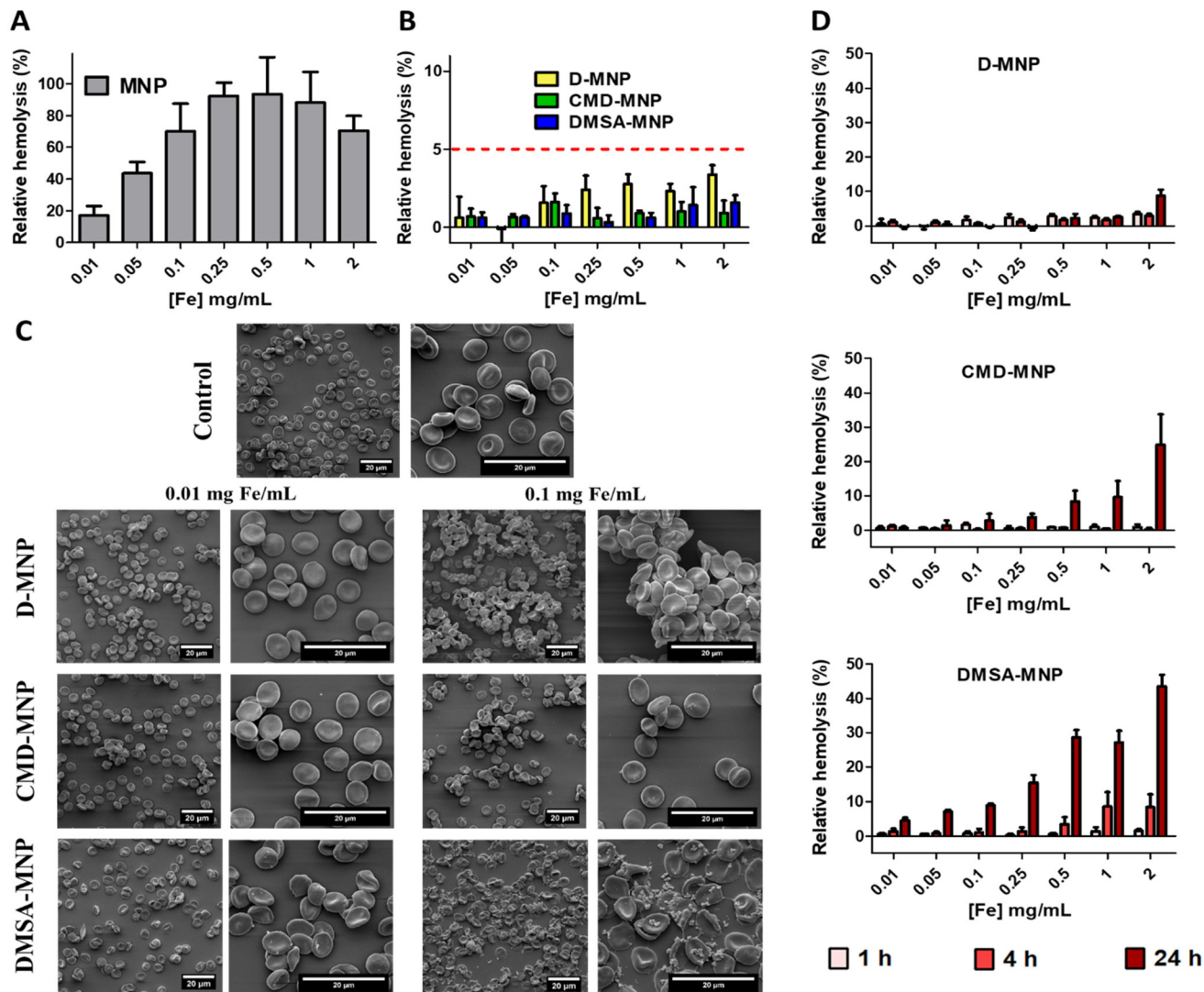


Fig. 1 Hemocompatibility studies of magnetic nanoparticles incubated with human red blood cells in PBS at 37 °C. (A) Hemolytic activity of MNP incubated with RBC at different concentrations for 1 h (mean \pm SD, $n = 4$). (B) Hemolytic activity of D-MNP, CMD-MNP and DMSA-MNP incubated with RBC at different concentrations for 1 h (mean \pm SD, $n = 4$). (C) SEM pictures of RBC incubated with D-MNP, CMD-MNP and DMSA-MNP at two concentrations (0.01 mg Fe per mL and 0.1 mg Fe per mL) for 1 h. Scale bar: 20 μ m. (D) Hemolytic activity of D-MNP, CMD-MNP and DMSA-MNP incubated with RBC at different concentrations for 1, 4 and 24 h (mean \pm SD, $n = 4$).

the rest of nanoparticles. Of note, although MNP interact less with plasma proteins (Fig. S3A–C[†]), big clusters of nanoparticles were formed (Fig. S3D[†]). It is possible that the plasma proteins enhance or stabilise the aggregation of MNP that already occurred in PBS (Fig. S2[†]). Thus, certain amount of plasma proteins were expected to be needed to magnify the formation of those big clusters. By contrary, the formation of those aggregates did not occur with the coated samples D-MNP and CMD-MNP, suggesting that these formulations are more suitable for biomedical applications in comparison both with MNP and DMSA-MNP. Overall, the results suggest that the interactions between nanoparticles and plasma proteins were highly influenced by the nature of their surface.

The previous results highlight the importance of coating MNP to ensure their biocompatibility with blood components.

However, further evaluations involving their interaction with macrophages are required to better understand the effects of our nanoparticles in animals. Thus, D-MNP, CMD-MNP and DMSA-MNP were employed for the studies with macrophages. These cells are specialized in sequestering inert particles,^{52,53} and they are also part of the tumor-infiltrating immune cells that modulate tumor progression.^{24,54}

Firstly, the cytocompatibility of the coated magnetic nanoparticles (0.01–0.5 mg Fe per mL) was assessed in the cell line of murine macrophages RAW 264.7 (Fig. 2A–C), and in the differentiated macrophages upon stimulation with PMA from the human cell line THP-1 (Fig. 2D–F) after 24, 48 and 72 h of incubation. The cytotoxicity of the coated magnetic nanoparticles was similar in all macrophages tested. DMSA-MNP presented more toxicity, especially remarkable at 0.25 and

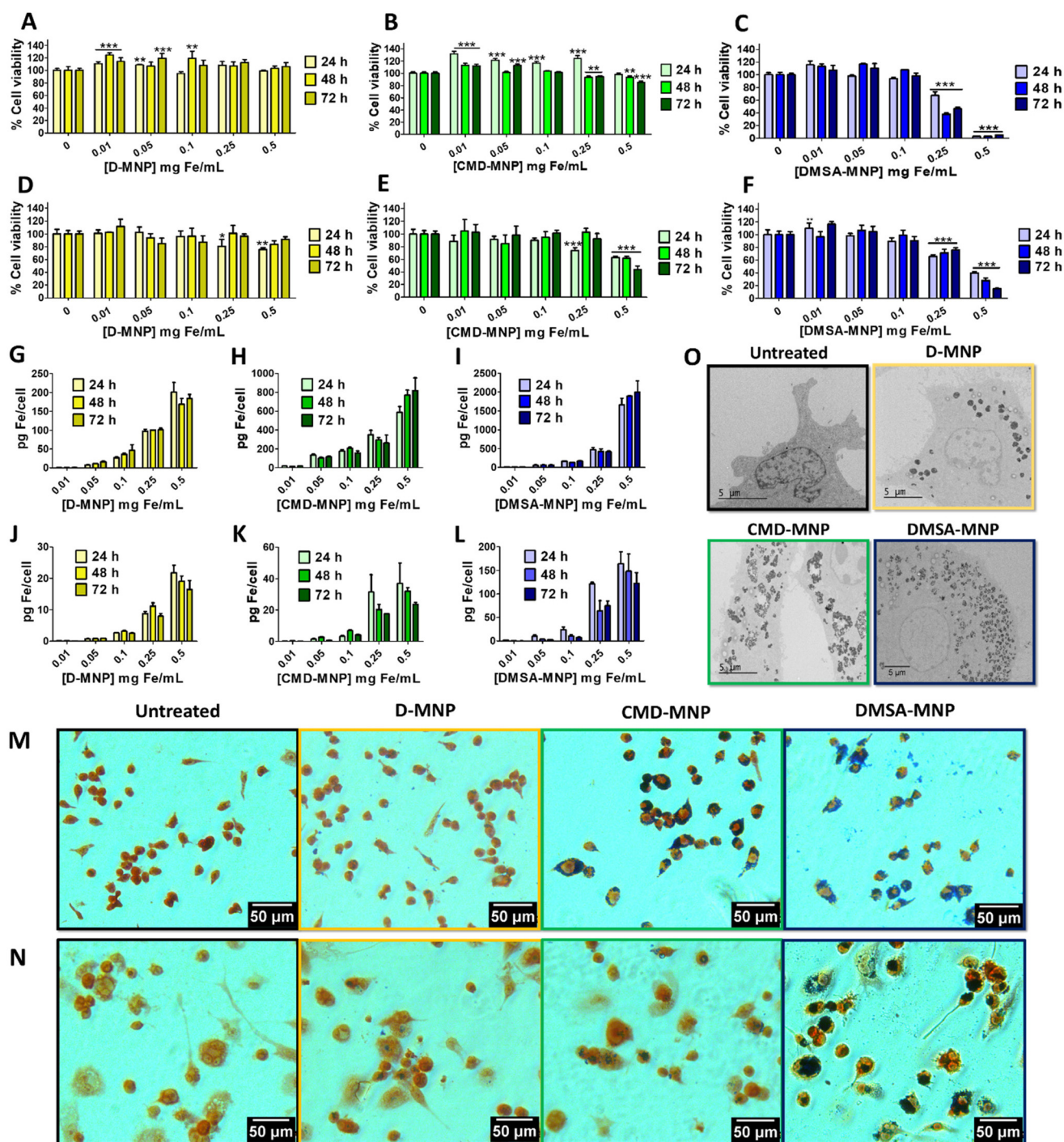


Fig. 2 Cell viability assays in RAW 264.7 (A-C) and THP-1 (D-F) cells after 24, 48 and 72 h of incubation with D-MNP (A, D), CMD-MNP (B, E) and DMSA-MNP (C, F) using CellTiterGlo. Data represent mean \pm SD ($n = 4$). Statistical analysis was performed using a one-way ANOVA test (each group vs. untreated condition). * $p < 0.05$, ** $p < 0.01$, *** $p < 0.001$. Ferrozine assays in RAW 264.7 (G-I) and THP-1 (J-L) cells after 24, 48 and 72 h of incubation with D-MNP (G, J), CMD-MNP (H, K) and DMSA-MNP (I, L). Data represent mean \pm SD ($n = 3$). Prussian Blue staining photos in RAW 264.7 (M) and THP-1 (N) cells after 48 h of treatment. TEM images of RAW 264.7 cells (O) untreated and incubated with D-MNP, CMD-MNP and DMSA-MNP for 48 h (scale bar: 5 μm).

0.5 mg Fe per mL (Fig. 2C and F), whereas D-MNP had negligible cytotoxicity at all concentrations tested (Fig. 2A and D). Lastly, CMD-MNP presented limited toxicity in murine macrophages (Fig. 2B) and they only significantly reduced the cell

viability at concentrations higher than 0.1 mg Fe per mL in THP-1 cells (Fig. 2F).

For a better understanding of the effects in the cell viability of coated MNP, their internalization was assessed by measur-

ing the iron content in cells 24, 48 and 72 h of incubation using the ferrozine method (Fig. 2G–L).⁵⁵ DMSA-MNP were the most internalized (Fig. 2I and L), followed by CMD-MNP (Fig. 2H and K) and, finally, D-MNP (Fig. 2G and J). These differences could be related to their surface charge and chemical composition,^{56,57} and might also be associated with their toxicity. Complementarily, the Prussian blue staining (0.1 mg Fe per mL) (Fig. 2M and N) revealed that the nanoparticles seemed to be localized in the cytoplasm without entering the nucleus, which was also confirmed by observing them inside cytoplasmic vesicles by TEM (Fig. 2O).

Lastly, to elucidate the internalization pathways involved, RAW 264.7 and THP-1 cells were incubated with classic endocytosis inhibitors⁵⁸ before adding the nanoparticles (0.1 mg Fe per mL) and the ferrozine assay was performed (Fig. S4†). Data suggest that macrophages internalized the nanoparticles mainly *via* clathrin-mediated endocytosis and macropinocytosis (Fig. S4†). Moreover, DMSA-MNP seem to be also internalized *via* caveolin-mediated endocytosis (Fig. S4C and S4F†). This additional mechanism of endocytosis involved in DMSA-MNP internalization could explain why they were better taken up than CMD-MNP although the differences in their surface charge were not significant (Table S4†). Thus, it might be related with DMSA composition.

Additionally, we evaluated if our nanoparticles triggered reactive oxygen species (ROS) production in the macrophages at non-toxic concentrations since some studies suggest that iron oxide nanoparticles can induce its generation^{24,52,53,59}

and iron overload might be related to M1 polarization by increasing ROS.⁶⁰ Surprisingly, our nanoparticles did not produce any exacerbation of ROS in any of the cell lines and incubation times tested (Fig. S5†). These results highlight the good biocompatibility of our nanoparticles with murine and human macrophages.

Finally, we evaluated if our nanoparticles had any effect on the cell cycle of macrophages by flow cytometry at the highest non-toxic concentration, 0.1 mg Fe per mL (Fig. S6†). The results suggest that coated MNP had a negligible effect on the cell cycle of THP-1 cells (Fig. S6D–F†). Similar results were obtained in RAW 264.7 (Fig. S6A–C†), although some differences could be observed in G2/M phase, especially with DMSA-MNP after 24 h and 48 h of incubation (Fig. S6A and S6B†), but they were not associated with differences in toxicity (Fig. 2C). Altogether, we considered that 0.1 mg Fe per mL was the optimum concentration to proceed with the immunostimulation studies since it was not related to cytotoxicity (Fig. 2A–F) or significant effects of the cell cycle (Fig. S6†).

To assess the possible contribution of coated MNP to the immunostimulation of macrophages, we evaluated the expression of CD80 and CD86 markers by flow cytometry (Fig. 3A–D) and the effect in the mRNA levels of TNF- α and IL-6 by RT-qPCR (Fig. 3E–H) in murine and human macrophages after 48 h of incubation. The expression of CD80 and CD86 surface markers has been extensively used to assess the potential immunostimulant role of nanoparticles^{45,61,62} since they are needed in the priming of naïve T-cells by antigen-pre-

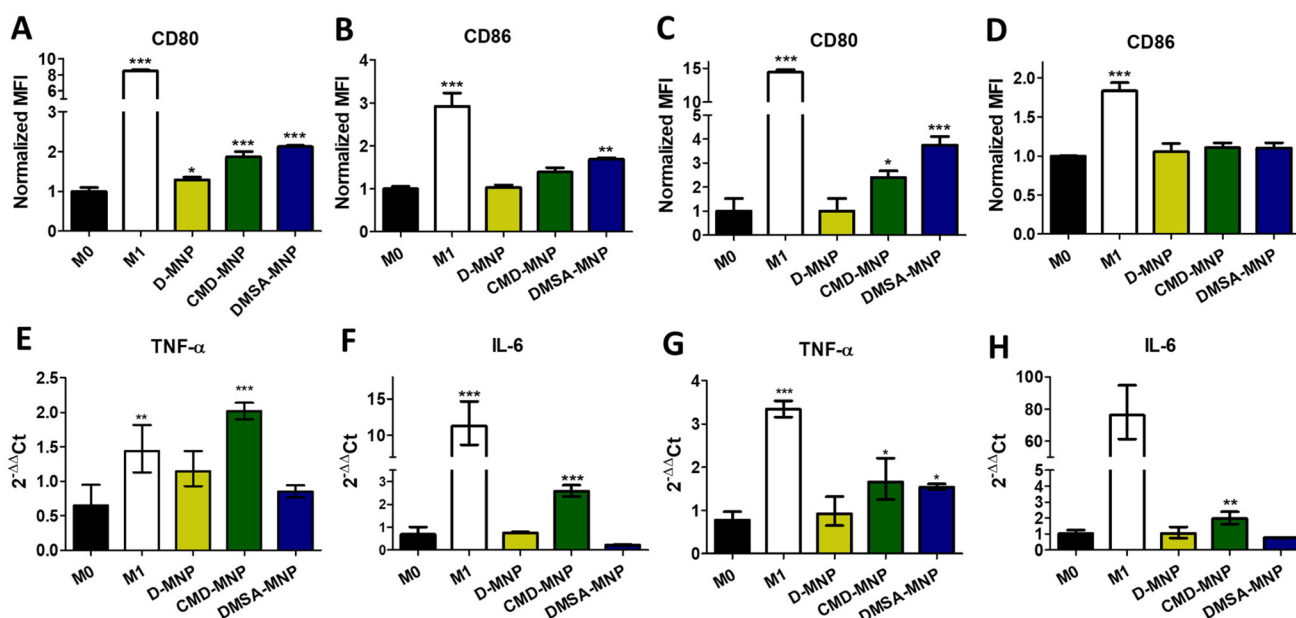


Fig. 3 Flow cytometry analysis of macrophage markers CD80 and CD86 expression in RAW 264.7 (A, B) and THP-1 (C, D) cells. TNF- α and IL-6 mRNA levels in RAW 264.7 (E, F) and THP-1 (G, H) macrophages were measured by RT-qPCR. For the calculation of $2^{-\Delta\Delta Ct}$ the Livak method was used and β -actin was employed as gene control. It is a relative quantification which relates the PCR signal of the target transcript in a treatment group to that of another sample such as an untreated control (in our case an additional M0 well). Data are presented as mean \pm SD ($n = 3$). For statistical analysis, one way ANOVA followed by Dunnett's post test was performed. * $p < 0.05$, ** $p < 0.01$, *** $p < 0.001$. The concentration of the nanoparticles for all the experiments was 0.1 mg Fe per mL.

senting cells in the lymph nodes.⁶³ Additionally, the induction of pro-inflammatory genes that contribute to M1 polarization⁶⁴ was assessed by checking mRNA levels of TNF- α and IL-6, two well-known pro-inflammatory cytokines.^{65,66}

On the one hand, the incubation of RAW 264.7 cells with the coated MNP led to an increase in the expression of the CD80 marker (Fig. 3A), and only DMSA-MNP significantly increased CD86 (Fig. 3B). On the other hand, CMD-MNP and especially DMSA-MNP increased CD80 marker expression, but no differences were observed in CD86 in THP-1 cells (Fig. 3C and D). Therefore, in both cell lines immunostimulant CD80 marker expression (Fig. 3A and C) might be triggered by iron oxide since the more internalization of MNP (Fig. 2G–L), the higher the levels observed. The expression of CD86 seemed to follow a similar pattern in RAW 264.7 cells (Fig. 3B), but not in THP-1 cells (Fig. 3D).

Regarding the effect of coated MNP in mRNA TNF- α and IL-6 levels, it is worth noting that CMD-MNP significantly increased their expression in both cell lines tested (Fig. 3E–H). By contrast, D-MNP had no effect, and DMSA-MNP only significantly increased mRNA TNF- α expression in THP-1 cells (Fig. 3G). Consequently, the contribution of iron seems less likely to explain the effect of the coated MNP, but the nature of the coating appeared to be crucial in triggering the mRNA expression of these pro-inflammatory cytokines. Thus, CMD might contribute to that end (Fig. 3E–H).

Considering the above results, CMD-MNP was selected as the best candidate for the functionalization with miRNA for the excellent results in terms of hemocompatibility (Fig. 1) and their limited interaction with plasma proteins (Fig. S3[†]). Additionally, they were better internalized than D-MNP in macrophages (Fig. 2G–O), less toxic than DMSA-MNP (Fig. 2A–F), and they presented immunomodulatory properties towards an M1 state (Fig. 3).

Three microRNAs were conjugated to CMD-MNP: miRNA-155, miRNA-125b and miRNA-146a (Fig. 4A). miRNA-155 and miRNA-125b were expected to contribute to the M1 polarization of macrophages,^{25,29} whereas miRNA-146a was employed as a control for its opposite effect.^{31,32} The amount of oligonucleotide attached was determined by quantifying the 2-pyridinethione released to the medium during the functionalization process. In all cases, 2.5 μ mol of oligonucleotide per g of Fe were bonded (5 μ M at 2 mg Fe per mL). The attachment of the oligonucleotides to CMD-MNP was associated with an increase in the hydrodynamic size and a negative ζ -potential (Table S5[†]), which could be related to the presence of phosphates groups in the sequences.

Importantly, the modified nanoparticles (0.1 mg Fe per mL, 0.25 μ M oligonucleotide) showed no cytotoxic effect (Fig. 4B). They presented similar internalization than CMD-MNP (Fig. 4C), and they were not associated with ROS production (Fig. 4D) in THP-1 macrophages. Additionally, using a labeled

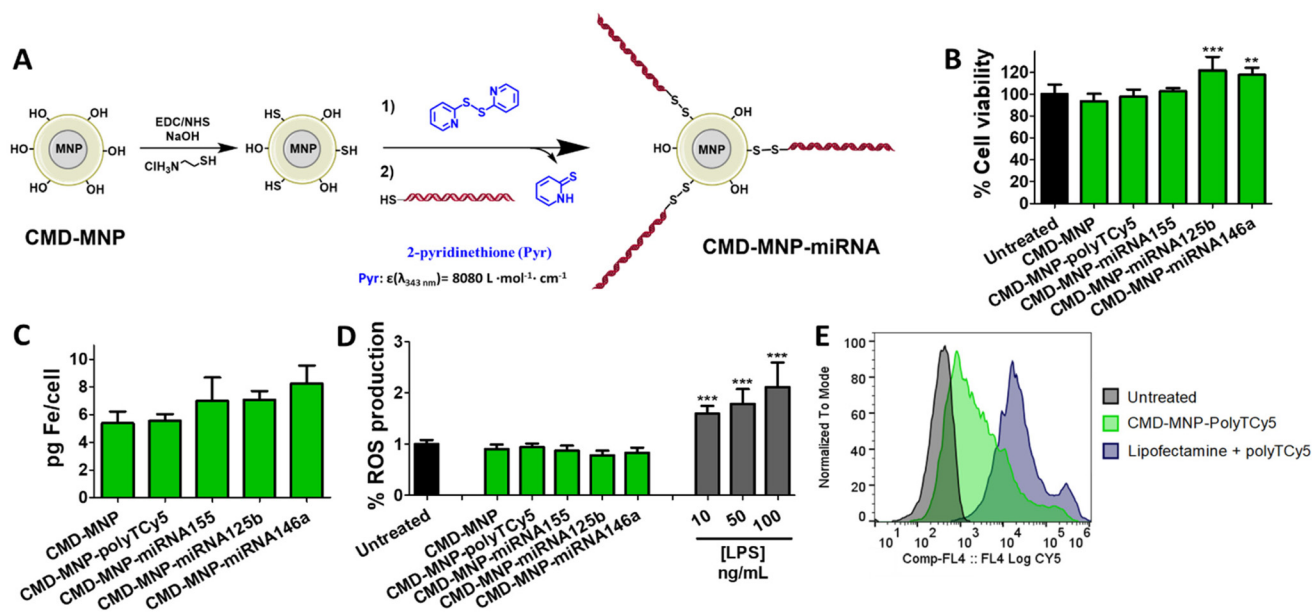


Fig. 4 (A) General scheme of functionalization of CMD-MNP with oligonucleotides *via* disulfide bonds. (B) Cell viability assays in THP-1 macrophages after 48 h of incubation with CMD-MNP and oligonucleotide-functionalized CMD-MNP. Data represent mean \pm SD ($n = 4$). (C) Ferrozine assays of CMD-MNP and oligonucleotide-functionalized CMD-MNP in THP-1 macrophages. Data represent mean \pm SD ($n = 3$). (D) Quantification of ROS levels in THP-1 macrophages by the detection of oxidized DCF-DA 48 h after treatment with CMD-MNP and oligonucleotide-functionalized CMD-MNP. Data represent mean \pm SD ($n = 6$). (E) Flow cytometry analysis of CMD-MNP-polyTCy5 internalization in THP-1 macrophages. Transfected cells with lipofectamine were used as a positive control. Statistical analysis was performed using a one-way ANOVA test (each group vs. untreated condition). ** $p < 0.01$, *** $p < 0.001$. The concentration of the nanoparticles for all the experiments was 0.1 mg Fe per mL and 0.25 μ M oligonucleotide (polyTCy5, miRNA155, miRNA125b or miRNA146a).

oligonucleotide (PolyTCy5) the internalization of oligonucleotides inside cells was studied by flow cytometry (Fig. 4E).

Moreover, we studied the effect of the miRNA-functionalized CMD-MNP on CD80 and CD86 by analyzing the cell surface markers expression (Fig. 5A and B), the mRNA levels of TNF- α and IL-6 (Fig. 5C and D) and intracellular levels of miRNA155 and miRNA125b (Fig. 5E and F) in THP-1 macrophages after 48 h of incubation.

According to our results, both CMD-MNP-miRNA155 and CMD-MNP-miRNA125b increased the expression of CD80 (Fig. 5A), but no CD86 (Fig. 5B). On the contrary, CMD-MNP-miRNA146a did not affect the surface markers expression (Fig. 5A and B). What is more interesting is that CMD-MNP-miRNA155 and CMD-MNP-miRNA125b increased more the expression of CD80 in comparison with the carrier (CMD-MNP) or the transfected miRNAs with lipofectamine (lipo miRNA155, lipo miRNA 125b), and the corresponding negative control (CMD-MNP-miRNA146a, lipo miRNA146a) (Fig. 5A). These results suggest a synergistic effect between the CMD-MNP and the miRNA155 (CMD-MNP-miRNA155), since its effect is higher than just the combined effect observed for the nanoparticles (CMD-MNP) and the transfected miRNA155 with lipofectamine (lipo miRNA155). In the case of CMD-MNP-miRNA125b, a combined response was identified (Fig. 5A).

Attending to the results of mRNA TNF- α levels, it is worth noting that CMD-MNP-miRNA125b treatment was associated with similar mRNA levels than the M1 control, and the effect of CMD-MNP-miRNA155 was similar to CMD-MNP (Fig. 5C).

Moreover, miRNA155 and miRNA125b transfected with lipofectamine did not display the same effect (Fig. 5C). By contrast, mRNA IL-6 levels were increased in the presence of those miRNAs (lipo miRNA155, lipo miRNA125b) and that effect was even magnified with CMD-MNP-miRNA155 and CMD-MNP-miRNA125b (Fig. 5D), being in both cases higher than the sum of the individual effects of CMD-MNP and lipofectamine transfected miRNAs (lipo miRNA155, lipo miRNA125b).

It is worth mentioning that miRNA155 (Fig. 5E) and miRNA125b (Fig. 5F) were overexpressed in M1 macrophages compared to M0, suggesting that they are implicated in the pro-inflammatory response (Fig. 5E and F). In this regard, despite the higher increase of these miRNAs achieved by lipofectamine, their induction of CD80, TNF- α and IL-6, it is much less pronounced than the formulations containing CMD-MNP-miRNA. Therefore, the synergistic effects mentioned before are clearly due to the combination of the nanoparticle and the pro-inflammatory miRNAs.

Of note, the effects observed by the oligonucleotide-modified nanoparticles suggest that the miRNAs were efficiently released due to the internal reducing environment of macrophages and the disulfide moiety used in the linker. On the one hand, the release was expected due to the adapted endocytic pathway of macrophages for the processing of protein-based antigens whose disulfide bonds need to be broken^{40,41} On the other hand, the disulfide bond employed in the linkage ease the intracellular controlled release of the miRNAs,⁶⁷ which are internalized thanks to the nanoparticle. In this regard, the

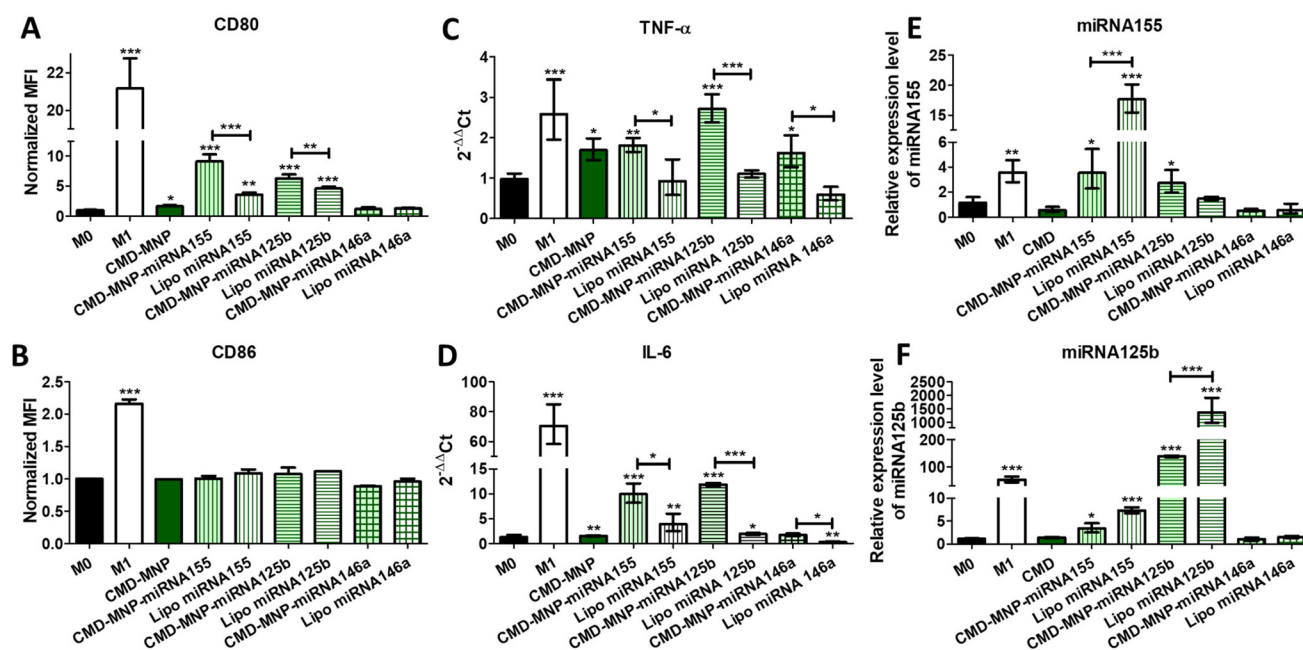


Fig. 5 Flow cytometry analysis of macrophage markers CD80 (A) and CD86 (B) expression in THP-1 macrophages. TNF- α (C) and IL-6 (D) mRNA levels in THP-1 macrophages were measured by RT-qPCR. For the calculation of $2^{-\Delta\Delta Ct}$ we used Livak method and β -actin was employed as gene control. miRNA155 (E) and miRNA125b (F) relative expression was calculated using Livak method, miRNA-423-5p was used as control and data was normalized with an untreated control. Data in C, D, E, F is presented as mean \pm SD ($n = 3$). For statistical analysis, one way ANOVA followed by Dunnett's post test was performed. * $p < 0.05$, ** $p < 0.01$, *** $p < 0.001$. The concentration of the nanoparticles for all the experiments was 0.1 mg Fe per mL and 0.25 μ M oligonucleotide (miRNA155, miRNA125b or miRNA146a).

nanof ormulation helps to overcome the repulsive forces with the hydrophobic and negatively charged cell membrane,^{68,69} leading to the optimal accumulation of the bioactive nanoparticles inside the cells.

Despite the promising results obtained with the current formulations, it is worth mentioning that the dosage of miRNAs included in our proposed CMD-MNP carrier can be modulated to optimize the amount of miRNA needed to trigger the desired pro-inflammatory effect. Thus, to optimize the performance of our proposed nanocarrier, the desired levels of each miRNA for a particular application must be investigated. Additionally, the loading capacity of the nanoparticles can be improved by chemically modifying the CMD to make the reactive groups more accessible, and with the introduction of stabilizing molecules (*e.g.*, PEG) to increase their colloidal stability.

Conclusions

In conclusion, we have synthesized, characterized, and evaluated the biocompatibility with blood components of magnetic nanoparticles composed of a maghemite core (MNP) and different coatings. The results suggest that the coating is indispensable to ensure the integrity of RBCs and, although it is related to an increase in the adhesion of plasma proteins, the resulting protein corona is not associated with the formation of larger aggregates. Additionally, we have demonstrated that the immunotoxicity and internalization of the nanoparticles in murine and human macrophages are highly influenced by their surface charge and the chemical composition of the coating. Importantly, the nanoparticles displayed a pro-inflammatory effect on macrophages independent of ROS production. Thus, other mechanisms, *e.g.*, autophagy or changes in the iron metabolism, could be involved.^{24,52,70} By comparing the three coated MNP, we concluded that CMD-MNP was the most promising candidate in terms of biosafety and immunomodulatory properties. Hence, a smart miRNA delivery system based on disulfide bonds using CMD-MNP as a carrier is proposed. Particularly, miRNA155 and miRNA125b (two miRNA whose production is exacerbated in an inflammatory response^{25,29}) were effectively delivered and their effect in pro-inflammatory cell surface marker CD80 and cytokine gene levels (TNF- α and IL-6) was magnified when they were internalized with CMD-MNP in human macrophages (THP-1). Hence, we have proved in human macrophages the potential of magnetic nanoparticles for immunotherapeutic applications in cancer, where a pro-inflammatory response is needed,²⁴ by taking advantage of their intrinsic properties and their easy functionalization with miRNAs. Overall, our studies provide insights on the potential of magnetic nanoparticles for their use in biomedical applications at different levels, including their biosafety profile and immunomodulatory properties in macrophages. Of note, this is the first time that magnetic nanoparticles have been proposed and broadly studied for the delivery of miRNA to polarize macrophages.

Experimental

The details on materials and methods can be found in the ESI.†

Author contributions

N. L. G.: conceptualization, data curation, formal analysis, investigation, methodology, visualization, writing-original draft. S. W., F. F., M. D., D. G.-S., A. C., M. C., C. R. D., G. S. investigation, resources, writing-review and editing. H. A. S. and Á. S.: conceptualization, methodology, writing-review and editing, funding acquisition, supervision and project administration.

Conflicts of interest

There are no conflicts to declare.

Acknowledgements

This work was supported by the Spanish Ministry of Economy and Competitiveness (SAF2017-87305-R, PID2020-119352RB-I00, PID2019-106301RB-I00), Comunidad de Madrid (IND2017/IND-7809; S2017/BMD-3867, IND2020/IND-17517), Asociación Española Contra el Cáncer, and IMDEA Nanociencia. IMDEA Nanociencia acknowledges support from the 'Severo Ochoa' Programme for Centres of Excellence in R&D (MINECO, Grant SEV-2016-0686, CEX2020-001039-S). This project has received funding from the European Union's Horizon 2020 research and innovation programme under grant agreement No 685795 (NoCanTher). We also acknowledge the European Structural and Investment Fund. Nuria Lafuente-Gómez also thanks the Spanish Education Ministry (FPU18/02323), the Spanish Ministry of Universities (EST19/00098) and the group of Jóvenes Investigadores Químicos (JIQ) from Spanish Royal Society of Chemistry (RSEQ) for the funding. Shiqi Wang acknowledges the financial support from Finnish Culture Foundation (grant no. 00201144) and from Academy of Finland (decision no. 331106). Hélder A. Santos acknowledges the financial support from the Sigrid Jusélius Foundation, the Academy of Finland (decision no. 331151), and the UMCG Research Funds.

References

- 1 J. P. Martins, J. das Neves, M. de la Fuente, C. Celia, H. Florindo, N. Günday-Türelı, A. Papat, J. L. Santos, F. Sousa, R. Schmid, J. Wolfram, B. Sarmento and H. A. Santos, *Drug Delivery Transl. Res.*, 2020, **10**, 726–729.
- 2 B. Sarmento and S. Little, *Drug Delivery Transl. Res.*, 2020, **10**, 571.
- 3 A. A. Gabizon, R. T. M. de Rosales and N. M. La-Beck, *Adv. Drug Delivery Rev.*, 2020, **158**, 140–157.

- 4 N. Lafuente-Gómez, A. Latorre, P. Milán-Rois, C. R. Diaz and Á. Somoza, *Chem. Commun.*, 2021, **57**, 13662–13677.
- 5 J. Jeevanandam, A. Barhoum, Y. S. Chan, A. Dufresne and M. K. Danquah, *Beilstein J. Nanotechnol.*, 2018, **9**, 1050–1074.
- 6 A. M. Ealias and M. P. Saravanakumar, in *IOP Conference Series: Materials Science and Engineering*, Institute of Physics Publishing, 2017, vol. 263, p. 032019.
- 7 H. A. Khan, M. K. Sakharkar, A. Nayak, U. Kishore and A. Khan, in *Nanobiomaterials: Nanostructured Materials for Biomedical Applications*, Elsevier Inc., 2018, pp. 357–384.
- 8 D. Stanicki, L. Vander Elst, R. N. Muller and S. Laurent, *Curr. Opin. Chem. Eng.*, 2015, **8**, 7–14.
- 9 D. García-Soriano, P. Milán-Rois, N. Lafuente-Gómez, C. Navío, L. Gutiérrez, L. Cussó, M. Desco, D. Calle, Á. Somoza and G. Salas, *J. Colloid Interface Sci.*, 2022, **613**, 447–460.
- 10 A. LeBrun and L. Zhu, in *Theory and Applications of Heat Transfer in Humans*, John Wiley & Sons Ltd, Chichester, UK, 2018, pp. 631–667.
- 11 A. Farzin, S. A. Etesami, J. Quint, A. Memic and A. Tamayol, *Adv. Healthcare Mater.*, 2020, **9**, 1901058.
- 12 D. García-Soriano, R. Amaro, N. Lafuente-Gómez, P. Milán-Rois, Á. Somoza, C. Navío, F. Herranz, L. Gutiérrez and G. Salas, *J. Colloid Interface Sci.*, 2020, **578**, 510–521.
- 13 N. Lafuente-Gómez, P. Milán-Rois, D. García-Soriano, Y. Luengo, M. Cordani, H. Alarcón-Iniesta, G. Salas and Á. Somoza, *Cancer*, 2021, **13**, 4095.
- 14 A. Latorre, P. Couleaud, A. Aires, A. L. Cortajarena and Á. Somoza, *Eur. J. Med. Chem.*, 2014, **82**, 355–362.
- 15 A. Aires, S. M. Ocampo, B. M. Simões, M. Josefa Rodríguez, J. F. Cadenas, P. Couleaud, K. Spence, A. Latorre, R. Miranda, Á. Somoza, R. B. Clarke, J. L. Carrascosa and A. L. Cortajarena, *Nanotechnology*, 2016, **27**, 1–10.
- 16 S. Kossatz, J. Grandke, P. Couleaud, A. Latorre, A. Aires, K. Crosbie-Staunton, R. Ludwig, H. Dähring, V. Ettelt, A. Lazaro-Carrillo, M. Calero, M. Sader, J. Courty, Y. Volkov, A. Prina-Mello, A. Villanueva, Á. Somoza, A. L. Cortajarena, R. Miranda and I. Hilger, *Breast Cancer Res.*, 2015, **17**, 1–17.
- 17 S. Persano, P. Das and T. Pellegrino, *Cancer*, 2021, **13**, 2735.
- 18 L. P. Wu, D. Wang and Z. Li, *Mater. Sci. Eng., C*, 2020, **106**, 110302.
- 19 G. Hannon, J. Lysaght, N. J. Liptrott and A. Prina-Mello, *Adv. Sci.*, 2019, **6**, 1900133.
- 20 J. Galon and D. Bruni, *Immunity*, 2020, **52**, 55–81.
- 21 A. Mantovani, P. Allavena, A. Sica and F. Balkwill, *Nature*, 2008, **454**, 436–444.
- 22 M. Pittet, O. Michielin and D. Mingliorini, *Nat. Rev. Clin. Oncol.*, 2022, **19**, 402–421.
- 23 X. Li, R. Liu, X. Su, Y. Pan, X. Han, C. Shao and Y. Shi, *Mol. Cancer*, 2019, **18**, 1–16.
- 24 V. Mulens-Arias, J. M. Rojas and D. F. Barber, *Front. Immunol.*, 2021, **12**, 1–14.
- 25 J. Raisch, A. Darfeuille-Michaud and H. T. T. Nguyen, *World J. Gastroenterol.*, 2013, **19**, 2985.
- 26 Y. Xing, Z. Wang, Z. Lu, J. Xia, Z. Xie, M. Jiao, R. Liu and Y. Chu, *Immunother. Adv.*, 2021, **1**, 1–13.
- 27 M. Bhaskaran and M. Mohan, *Vet. Pathol.*, 2014, **51**, 759–774.
- 28 V. Scalavino, M. Liso and G. Serino, *Int. J. Mol. Sci.*, 2020, **21**, 1–18.
- 29 E. Tili, J.-J. Michaille, A. Cimino, S. Costinean, C. D. Dumitru, B. Adair, M. Fabbri, H. Alder, C. G. Liu, G. A. Calin and C. M. Croce, *J. Immunol.*, 2007, **179**, 5082–5089.
- 30 W. Diao, L. Lu, S. Li, J. Chen, K. Zen and L. Li, *Biochem. Biophys. Res. Commun.*, 2017, **491**, 912–918.
- 31 K. D. Taganov, M. P. Boldin, K.-J. Chang and D. Baltimore, *Proc. Natl. Acad. Sci. U. S. A.*, 2006, **103**, 12481–12486.
- 32 M. L. Squadrito, M. Etzrodt, M. De Palma and M. J. Pittet, *Trends Immunol.*, 2013, **34**, 350–359.
- 33 M. A. Cortez, S. Anfossi, R. Ramapriyan, H. Menon, S. C. Atalar, M. Aliru, J. Welsh and G. A. Calin, *Genes Chromosom. Cancer*, 2019, **58**, 244–253.
- 34 K. B. Long and G. L. Beatty, *OncoImmunology*, 2013, **2**, 1–9.
- 35 A. Ahmad, *Semin. Cell Dev. Biol.*, 2021, 1–8.
- 36 A. Latorre and A. Somoza, *Curr. Top. Med. Chem.*, 2015, **14**, 2662–2671.
- 37 X. Guo, Y. Cheng, X. Zhao, Y. Luo, J. Chen and W.-E. Yuan, *J. Nanobiotechnol.*, 2018, **16**, 1–10.
- 38 S. Hirosue, I. C. Kourtis, A. J. van der Vlies, J. A. Hubbell and M. A. Swartz, *Vaccine*, 2010, **28**, 7897–7906.
- 39 F. Fontana, D. Liu, J. Hirvonen and H. A. Santos, *Wiley Interdiscip. Rev.: Nanomed. Nanobiotechnol.*, 2017, **9**, e1421.
- 40 P. Cresswell, B. Arunachalam, N. Bangia, T. Dick, G. Diedrich, E. Hughes and M. Maric, *Immunol. Res.*, 1999, **19**, 191–200.
- 41 R. L. Lackman, A. M. Jamieson, J. M. Griffith, H. Geuze and P. Cresswell, *Traffic*, 2007, **8**, 1179–1189.
- 42 R. Massart, *IEEE Trans. Magn.*, 1981, **17**, 1247–1248.
- 43 T. Liu, R. Bai, H. Zhou, R. Wang, J. Liu, Y. Zhao and C. Chen, *RSC Adv.*, 2020, **10**, 7559–7569.
- 44 T. L. Moore, L. Rodriguez-Lorenzo, V. Hirsch, S. Balog, D. Urban, C. Jud, B. Rothen-Rutishauser, M. Lattuada and A. Petri-Fink, *Chem. Soc. Rev.*, 2015, **44**, 6287–6305.
- 45 S. Wang, S. Wannasarit, P. Figueiredo, G. Molinaro, Y. Ding, A. Correia, L. Casettari, R. Wiwattanapatapee, J. Hirvonen, D. Liu, W. Li and H. A. Santos, *Adv. Ther.*, 2021, **4**, 2000058.
- 46 M. A. Shahbazi, M. Hamidi, E. M. Mäkilä, H. Zhang, P. V. Almeida, M. Kaasalainen, J. J. Salonen, J. T. Hirvonen and H. A. Santos, *Biomaterials*, 2013, **34**, 7776–7789.
- 47 Z. Karimi, L. Karimi and H. Shokrollahi, *Mater. Sci. Eng., C*, 2013, **33**, 2465–2475.
- 48 K. M. de la Harpe, P. P. D. Kondiah, Y. E. Choonara, T. Marimuthu, L. C. du Toit and V. Pillay, *Cells*, 2019, **8**, 1–25.
- 49 J. Wolfram, Y. Yang, J. Shen, A. Moten, C. Chen, H. Shen, M. Ferrari and Y. Zhao, *Colloids Surf., B*, 2014, **124**, 17–24.
- 50 D. Baimanov, R. Cai and C. Chen, *Bioconjugate Chem.*, 2019, **30**, 1923–1937.

- 51 C. Carrillo-Carrion, M. Carril and W. J. Parak, *Curr. Opin. Biotechnol.*, 2017, **46**, 106–113.
- 52 J. M. Rojas, L. Sanz-Ortega, V. Mulens-Arias, L. Gutiérrez, S. Pérez-Yagüe and D. F. Barber, *Nanomedicine*, 2016, **12**, 1127–1138.
- 53 C. F. Borgognoni, J. H. Kim, V. Zucolotto, H. Fuchs and K. Riehemann, *Artif. Cells, Nanomed., Biotechnol.*, 2018, **46**, 694–703.
- 54 Y. Yang, J. Guo and L. Huang, *Trends Pharmacol. Sci.*, 2020, **41**, 701–714.
- 55 J. Riemer, H. H. Hoepken, H. Czerwinska, S. R. Robinson and R. Dringen, *Anal. Biochem.*, 2004, **331**, 370–375.
- 56 A. Villanueva, M. Cañete, A. G. Roca, M. Calero, S. Veintemillas-Verdaguer, C. J. Serna, M. P. Morales and R. Miranda, *Nanotechnology*, 2009, **20**, 115103.
- 57 S. Salatin, S. Maleki Dizaj and A. Yari Khosroushahi, *Cell Biol. Int.*, 2015, **39**, 881–890.
- 58 G. N. Basturea, *Mater. Methods*, 2019, **9**, 2752.
- 59 O. Lunov, T. Syrovets, B. Büchele, X. Jiang, C. Röcker, K. Tron, G. U. Nienhaus, P. Walther, V. Mailänder, K. Landfester and T. Simmet, *Biomaterials*, 2010, **31**, 5063–5071.
- 60 Y. Zhou, K.-T. Que, Z. Zhang, Z. J. Yi, P. X. Zhao, Y. You, J.-P. Gong and Z.-J. Liu, *Cancer Med.*, 2018, **7**, 4012–4022.
- 61 F. Fontana, M. A. Shahbazi, D. Liu, H. Zhang, E. Mäkilä, J. Salonen, J. T. Hirvonen and H. A. Santos, *Adv. Mater.*, 2017, **29**, 1603239.
- 62 X. Fu, J. Yu, A. Yuan, L. Liu, H. Zhao, Y. Huang, S. Shen, F. Lv and S. Wang, *Chem. Commun.*, 2021, **57**, 6919–6922.
- 63 K. K. Wong, W. A. Li, D. J. Mooney and G. Dranoff, *Adv. Immunol.*, 2016, **130**, 191–249.
- 64 H. Peng, D. Xian, J. Liu, S. Pan, R. Tang and J. Zhong, *J. Immunol. Res.*, 2020, **2020**, 1–13.
- 65 Y. Luo and S. G. Zheng, *Front. Immunol.*, 2016, **7**, 1–7.
- 66 P. J. Murray, *Annu. Rev. Physiol.*, 2017, **79**, 541–566.
- 67 D. P. Bartel, *Cell*, 2004, **116**, 281–297.
- 68 I. Fernandez-Piñeiro, I. Badiola and A. Sanchez, *Biotechnol. Adv.*, 2017, **35**, 350–360.
- 69 M. Segal and F. J. Slack, *Expert Opin. Drug Discovery*, 2020, **15**, 987–992.
- 70 R. Jin, L. Liu, W. Zhu, D. Li, L. Yang, J. Duan, Z. Cai, Y. Nie, Y. Zhang, Q. Gong, B. Song, L. Wen, J. M. Anderson and H. Ai, *Biomaterials*, 2019, **203**, 23–30.